Spacetime Visualization of Relativistic Effects

Ping-Kang Hsiung*
Robert H. Thibadeau†
Carnegie Mellon University
Pittsburgh, Pennsylvania 15213

Abstract

We have developed an innovative ray-tracing algorithm to describe *R*elativistic *E*ffects in *S*pace*T*ime ("REST"). Our algorithm, called *REST-frame*, models light rays that have assumed infinite speed in conventional ray-tracing to have a *finite* speed c in spacetime, and uses general Lorentz Transformation, which connects the spacetime description of a single event in two inertial coordinate systems (*frames*) that differ by a constant velocity, to perform the relativistic translation and aberration of light rays.

In this paper, we report the extension of our previous work for visualizing relativistic motion in spacetime to include relativistic Doppler color shift and the simulation of complex kinematic systems in which objects of different relativistic velocities coexist. Our simulations have produced non-intuitive images showing anisotropic deformation (*warping*) of space and intensity concentration/spreading of light sources in spacetime. Images of objects undergoing relativistic Doppler shift are also generated.

By applying state-of-the-art computation technology and simulation techniques to the earlier quests in Physics that were conducted mainly by *thought experiment*, we demonstrate, through our new revelations, that *REST-frame* offers a powerful *experimentation tool* to study and explore some of the most exciting aspects of the natural world; particularly, the rich physical properties associated with the finite speed of light.

Keywords: Apparent effects of Special Relativity. Relativistic Doppler shift. Scientific visualization. Computer simulation. Computer image synthesis. Ray-tracing.

*Department of Electrical and Computer Engineering, Carnegie Mellon University. (412) 268-2524. pkh@cs.cmu.edu
†Imaging Systems Laboratory, The Robotics Institute, Carnegie Mellon University. rht@vi.ri.cmu.edu
This research was partially supported by Imaging Systems Laboratory, The Robotics Institute, Carnegie Mellon University.

1 Introduction

1.1 Motivations

The revival of interest in Special Relativity in the early 1960's was focused on the appearance of relativistic objects under *ad hoc* conditions. Until that time, for nearly fifty-five years since the inception of the special theory, such phenomena had not been fully explored.

Our intent today has been to produce simulation images with visual realism that incorporate the effects of

- object deformation due to relativistic spacetime geometry, and
- complete intra-object and inter-object optical phenomena, such as perspective projection, reflection, refraction and shadow casting.

Flexible selection of simulation parameters including viewpoint, viewing direction, viewing time and relative traveling velocity between objects and the observer is also essential. These requirements are accomplished by the application of an innovative ray-tracing algorithm, which we called *REST-frame*.

In this paper, we extend our previous work for visualizing one dimensional (1D) and three dimensional (3D) relativistic motion in spacetime to include a more general class of problems, in which the observed objects undergo *different* 3D motion relative to the observer. We also model the Doppler color shift due to relativistic motion.

1.2 Background and previous work

Einstein's Special Theory of Relativity (1905) postulated [12][13][9]:

1. Non-existence of preferred reference system (*"The Principle of Relativity"*): the laws of physics must be the same for observers in all inertial reference systems.[1]
2. Constancy of speed of light: c is constant in a vacuum in all inertial frames and is independent of the motion of a light source relative to the observer.

Some consequences of the spacetime model are:

[1] A reference system, or *reference frame*, is *inertial* in spacetime if it is nonaccelerating.

- The measured space and time coordinates are dependent upon the reference frame from which the measurement is made.
- The Lorentz Transformation relates measured spacetime coordinates between inertial reference frames.
- Lengths perpendicular to relative motion remain the same measurements for all inertial observers. Lengths parallel to relative motion are measured to have undergone contraction in comparison with their rest lengths.

James Terrell (1959)[14] made an early distinction between the *appearance* or visibility of relativistic effects and the *measurement* of relativistic effects. Following the initial work of Penrose (1959)[10] and Terrell, interest was sparked and a number of related papers were published.[2] The extent of this revival of interest was limited in that scientists lacked the computing power, ray-tracing technique, and visualization outlook.

Ray-tracing synthesizes images using a model that reverses the image formation process in nature [3][2](figure (1)). Rays are traced from pixels on the image plane through a

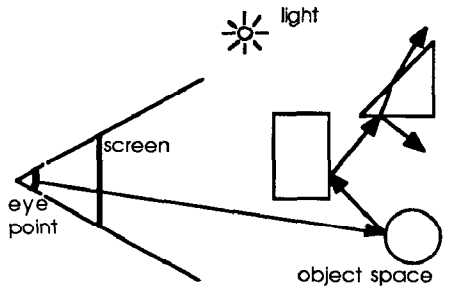

Figure 1: Ray-tracing principle

fixed "eye-point" (or "viewpoint") into the object space that forms the scene. Reflection and refraction rays ("secondary rays") are recursively spawned when rays meet (*"hit"*) objects. Light intensity is computed on the object surface at every ray-object intersection point according to some illumination model[11][17][15][1], and contributes to the final pixel intensity of the synthesized image.

This ray-tracing computation can be modeled as two interacting processes: the *intersection process* and the *shading process* (figure (2))[4]. The former solves for intersection points where rays hit scene object surfaces, while the latter performs shading computation.

In the traditional ray-tracing algorithms, a light ray had always been regarded as if it traveled with infinite speed, and Galilean-Newtonian transformation was used to model relative motion between dynamic systems and the observer. When the scene objects and the observer (or the camera plate) are in relative motion at speeds comparable to light speed, Special Relativity requires the time information to be interwoven with the spatial coordinates in defining the vision formation process. Light speed must be treated as *finite*, and reference frames are to be connected by Lorentz Transformation.

[2]Interested readers can find a more extensive bibliography in [5] about those papers as well as about research in ray-tracing simulation.

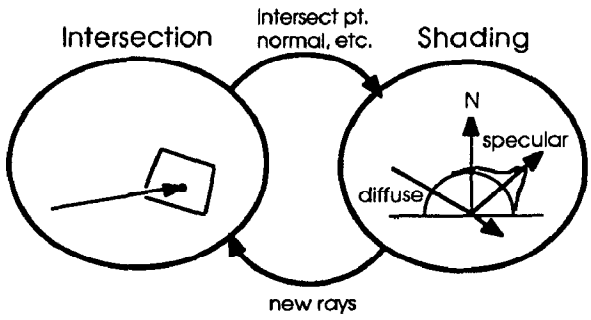

Figure 2: Ray-tracing computation model

In [5], we first treated the subject of visualizing the spacetime world of Special Relativity using the new ray-tracing technique *REST-frame*. Objects were assumed to make 1D motion relative to the observer. The 3D motion extension of our original work has since been completed[6]. A fast spacetime visualization method based on the scanline operation has also been designed and implemented[7].

2 Approach

2.1 *REST-frame* ray-tracing

The *REST-frame* technique synthesizes the visual effects in spacetime by incorporating the finite speed of light in ray-tracing to simulate the Special Relativity physics. Light-rays are traced back to their source events in the *past* in spacetime from the observation point, which is itself an event in spacetime. The three key elements in our approach are:

1. Time modeling in the ray-tracing equations: A ray that passes spacetime event[3] $[x_0, y_0, z_0, t_0]$ and travels in 3D direction $\vec{d}$ in a frame S is modeled as

$$r\vec{d}y_{REST} = (x, y, z) = (x(t_0),\ y(t_0),\ z(t_0)) + c(t_0 - t)\vec{d} \quad (t \le t_0) \qquad (1)$$

   Where t is the time the ray (traveling at light speed c) passes the coordinates (x, y, z) in S, starting at $[x_0, y_0, z_0, t_0]_S$.

2. Lorentz Transformation of rays between frames: For inertial Cartesian coordinate system $S'(x', y', z')$ with time t' that travels at a 3D velocity $\vec{V} = (u, v, w)$ relative to system $S(x, y, z)$ and t, if its X', Y' and Z' axes coincide with X, Y and Z, respectively, of S at time $t = t' = 0$, then the spatial and time coordinates[4] $\vec{X}'$ and t' can be derived from $\vec{X}$ and t in S using Lorentz Transformation[9]

$$\vec{X}' = \vec{X} + [\frac{(\gamma - 1)}{\| \vec{V} \|^2}(\vec{X} \cdot \vec{V}) - \gamma t]\vec{V}$$
$$t' = \gamma(t - \frac{\vec{X} \cdot \vec{V}}{c^2}) \qquad (2)$$

[3]We use the symbol (x, y, z) for 3D positional coordinates and $[x, y, z, t]$ for a spacetime event point. When we designate a specific reference frame S, we use $(x, y, z)_S$ and $[x, y, z, t]_S$. Individually, each component is written with a subscript S (e.g. t_S). We also use $[x_0, y_0, z_0, t_0]_S$ as a shorthand for spacetime event $[x(t_0), y(t_0), z(t_0), t_0]_S$, and $(x_0, y_0, z_0)_S$ for spatial point $(x(t_0), y(t_0), z(t_0))_S$.

[4]$\vec{X}' = (x', y', z')_{S'}$ and $\vec{X} = (x, y, z)_S$.

in which $\| \vec{V} \|^2 = u^2+v^2+w^2$, and $\gamma = 1/\sqrt{1 - \frac{\|\vec{V}\|^2}{c^2}}$. Vector $\vec{V}$ is sometimes replaced by vector $\vec{\beta} = (\beta_x, \beta_y, \beta_z) = (u/c, v/c, w/c)$.

For the ray in eq. (1), the S' representation of ray origin can be obtained by applying eq. (2) to the S frame origin $[x_0, y_0, z_0, t_0]_S$. This transformation has the effect that a ray *appears* to have its origin translated when moving from S to S'.

The ray direction $\vec{a}$ in S and $\vec{a'}$ in S' satisfy the following relativistic aberration equation:[5]

$$\vec{a'} = \frac{\vec{a} + [\frac{(\gamma-1)}{\|\vec{V}\|^2}(\vec{a} \cdot \vec{V}) + \gamma]\vec{V}}{\gamma(1 + \vec{a} \cdot \vec{V})} \quad (3)$$

3. Ray-object intersection in spacetime: For all objects that are in motion at a same speed relative to the image formation frame S, we can find a frame S' such that the objects are *stationary* in S',[6] and S' shares the three Cartesian coordinate axes with S at their common origin event $[0, 0, 0, 0]$.

   We transform screen rays defined ("fired") in S to their S' representations, and perform intersection test with the stationary objects in S'. Shade calculation and secondary rays spawning are also conducted conveniently in S'.

2.2 Multiple frame intersection

In order to extend the ray-object intersection method explained in section 2.1 to systems of objects with multiple velocities, it is necessary to consider multiple inertial frames S'_1, S'_2, ..., S'_n. Any object or group of objects which travels at a unique

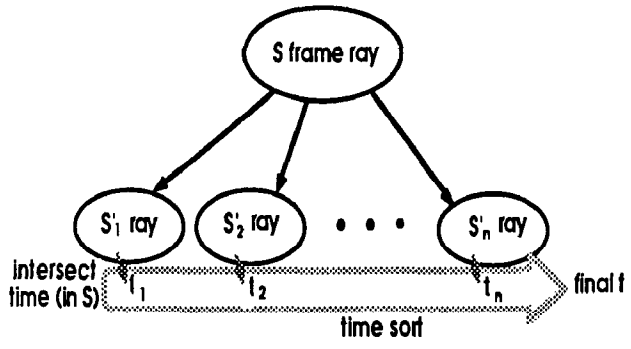

Figure 3: Multiple frame intersection and time sort

velocity with respect to observer frame S may be placed in its own proper frame S'_i. Our object space has thus been divided into a series of coexistent inertial frames. We then fire rays into all of the coexistent frames (figure 3). A given ray may result in one of three cases:

1. The ray misses all objects in all frames. The background color is returned, as is done for a "ray miss" in the conventional ray-tracing.
2. The ray hits one object at one spacetime event. The appropriate shade for that event is returned, again as was done previously.
3. The ray hits objects in more than one frames. This requires the hit events to be sorted in order of time in frame S, so that the most *recent* event is found; it is this event which is displayed.

The sort used in the third case is analogous to the *visibility sort* performed in conventional ray-tracing. In the latter, there is one single frame S'=S; any given hit event supersedes those that occurred before it in time.

We note that this multiple frame intersection method may be performed recursively, as is required for the computation of reflection and/or transmission of light in ray tracing. Each secondary ray, originated from a hit event in some S'_i, however, must be translated into the frames S'_1, S'_2, ..., S'_n for the reflected or transmitted event to be detected amongst the various inertial frames.

2.3 Relativistic Doppler effect

A light source in relativistic motion is *observed* to have a frequency shift according to the following formula:

$$f = \frac{1}{\gamma(1 + \vec{e} \cdot \vec{V})} f_o \quad (4)$$

The symbols used in equation (4) are

- f_o : *frequency of light in its proper frame S'.*
- f : *frequency of light observed in S.*
- $\vec{e}$: *observed direction of light in S.*
- $\vec{V}$: *Velocity of S' relative to S.*

The $\frac{1}{\gamma(1+\vec{e}\cdot\vec{V})}$ part is sometimes called the *Doppler shift factor.*

We implement the Doppler frequency shift effect by conducting the conventional ray-tracing shading in S' frame, and transforming the final color returned to each pixel[7] by its screen ray using eq. (4).

3 Implementation and experiments

3.1 Implementation

We have implemented this *REST-frame* ray-tracing approach based on the bounding volume intersection acceleration technique[8][5]. The scene objects are defined in an input file. Also included in the file are the viewpoint, view time, view angle and view direction parameters. For the multiple velocity simulations, we partition the objects by their frames, and specify their respective frame velocity independently. The light sources are assumed to be isotropic and stationary in the objects frame. We performed our experiments on an Apollo DN-10000 system with 2 CPU boards and 32M byte of physical memory. Most of our simulations took less than 5 minutes to produce 512 by 512 images, although for some complex scenes, the simulations exceeded 2 hours.

[5] See [12][9] for derivation.

[6] Such an S' is called the *proper frame* or *rest frame* for the objects.

[7] in observer frame S.

3.2 Experimental results

3.2.1 Headlamp effect

In the first set of experiments, we place a 2 x 2 array of light sources at a fixed distance in front of a diffusive plane. The plane and the light sources are in S' and move towards/away from the viewpoint in the viewing direction, which is perpendicular to the plane. Our results are shown in figures (4), (5), (6), (7), (8).

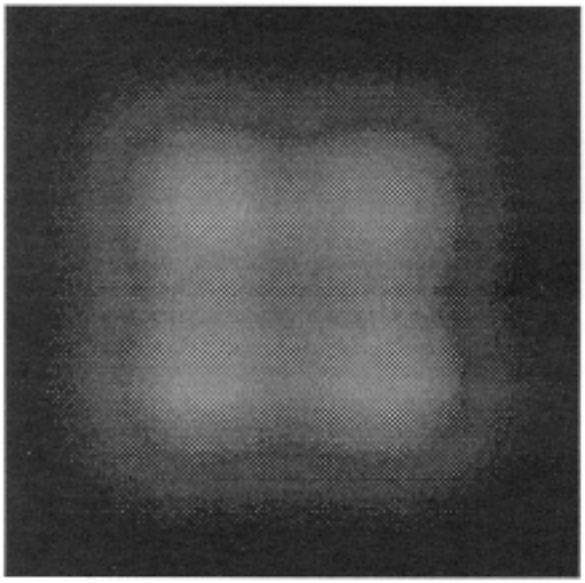

Figure 4: Light sources viewed at stationary (©1989 Hsiung)

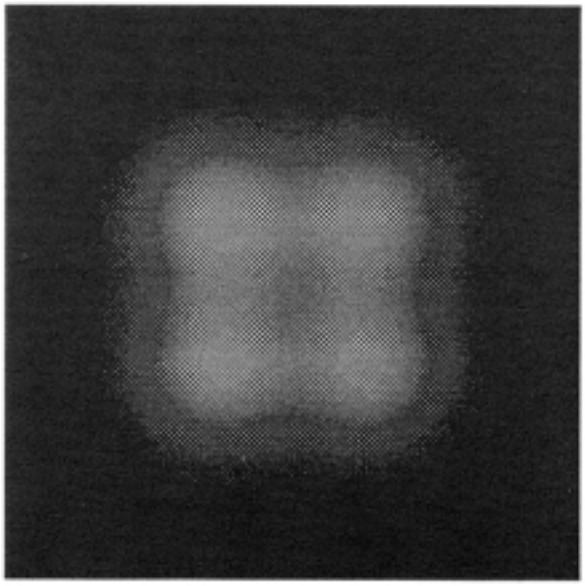

Figure 5: Light sources moving towards observer at 0.5c (©1989 Hsiung)

The imaging times in all figures are the same: the time when event [0, 0, 0, 0] arrives at the imaging plate. Therefore, the concentrating and flooding of light sources patterns revealed in these pictures are purely caused by the anisotropic warping of spacetime inherent in relativistic imaging, rather than by changing viewing configurations. This variation of light intensity distribution in space is termed *headlamp effect* in [16].[8]

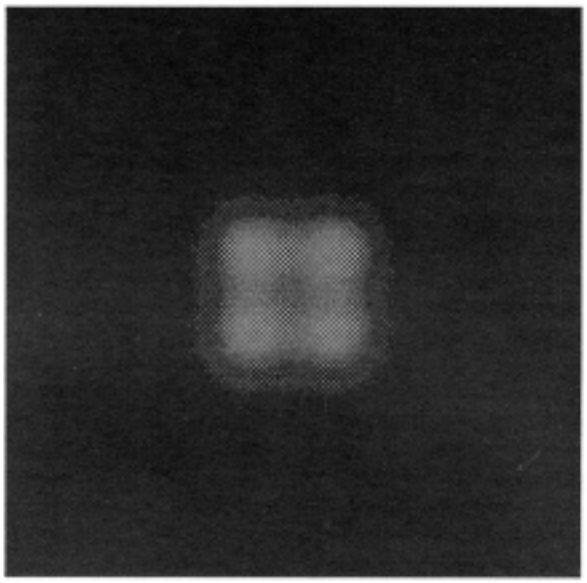

Figure 6: Light sources moving towards observer at 0.9c (©1989 Hsiung)

3.2.2 Multiple frame intersection

The second set of experiments has the scene configuration of an 11 x 11 array of bars, each aligned with the Z axis, spreading evenly on the X-Y plane in S'. The viewer is located at a fixed distance away on the positive Z axis in S, and looks towards the X-Y plane. Figure (9) shows the stationary image.

In figure (10), the bars travel in row formation in the X direction. The travel speeds of the bar rows increase from 0.0c at the bottom row to 0.9c at second to top row, in increment of 0.1c; the top row travels at 0.99c.

Figure (11) shows bar rows traveling in parallel to the +Z direction towards the observer. The middle row is moving at 0.95c, the rows next to it at 0.9c, and 0.7c, 0.5c, 0.3c, 0.0c subsequently. The lens-like effect[5] shows up with varying extent in rows due to the variation in traveling speed.

3.2.3 Relativistic Doppler effect

Our third set of experiments consists of a tile array that travels at various velocities in simulations. In each simulation, the Doppler shift factor in eq. (4) is computed at every pixel on the image plate. These numbers, rather than the absolute pixel color values, are then stored as the simulation output. To produce a final image, the output pixels are scaled and mapped to grayscale level of 0-255 in postprocessing. The scaling/mapping serves as a normalization process to increase the displayable dynamic range based on 256 grayscale levels; the resulting images thus show a *relative* measure of the Doppler shift.

Our results are shown in figures (12), (13), (14), and (15).

[8] We noticed that in *"Star-Trek IV"*, this effect was not done correctly.

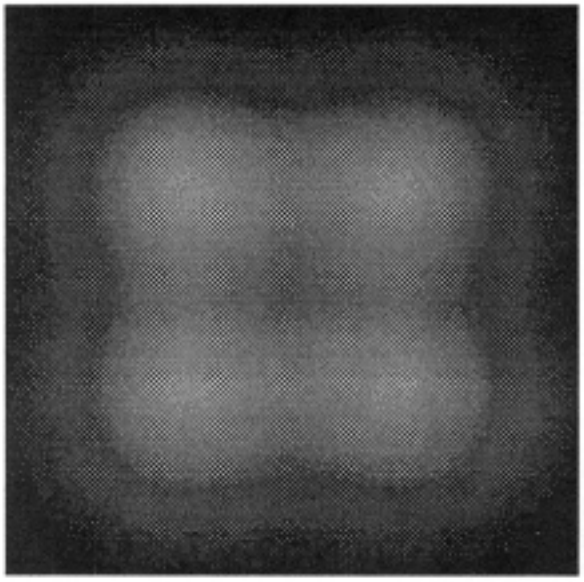

Figure 7: Light sources moving *away from* observer at 0.5c (©1989 Hsiung)

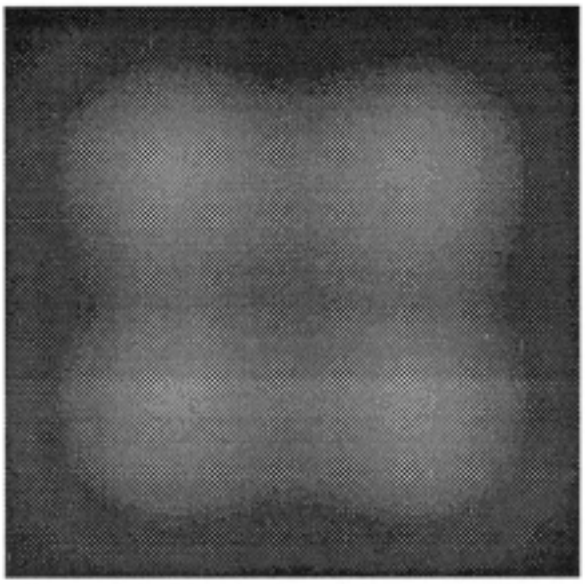

Figure 8: Light sources moving *away from* observer at 0.9c (©1989 Hsiung)

Figures (13) and (15) are, respectively, figures (12) and (14) quantized to 15 levels. We make the following remarks about these images:

- The brighter pixels represent higher Doppler shift levels, and the darker pixels the lower levels. The background portion of the images is from the void space, and is pseudo-colored to enhance the images.

  In the 0.8c sideways motion simulation, the range of the factors is (0.538, 0.703) – a red-shift over the entire image. A 0.9c sideways motion under the same viewing condition (images not shown) gives range of (0.398, 0.50), which is a narrower shift range. In the simulation of 0.9c objects motion towards the observer, the shift factor range is (3.407, 4.359).

- Figure (13) clearly shows the the concentric iso-Doppler-factor rings arisen from the symmetric spacetime geometry resulted from the relativistic motion. The central ring contains pixels of the highest shift factors.

- Figure (15) shows the interesting vertical stripes of iso-factor pixels. Each stripe covers pixels that have similar $(\vec{e} \cdot \vec{V})$ values.

4 Discussion

4.1 Possible extensions

We are making extensions of our current implementation in the following directions:

- A more complete light source model that incorporates moving light sources and self luminous bodies. Our current light sources are static in space and time.[9]

- A generalization to the current (constant and linear) motion model. Specifically, the modeling of acceleration and angular motion. In the first case, events at different pasts have different linear velocities. In the second case, points on a rotating object surface experiences different linear velocities relative to the viewer.

- Texture mapping — an element necessary to show, for instance, the surface feature distortion on a fast moving planet.

4.2 Color shift

In this paper, we have chosen to show the relative (normalized) scalar values of the Doppler shift factor, instead of the absolute RGB color images of the Doppler effect. To perform the latter approach, these following issues are involved:

- The surface properties of the objects need to be represented in the language of power spectral density, instead of the commonly used RGB or XYZ values.

- Dynamic range re-normalization: The Doppler shift in the more interesting motion conditions tends to be so severe (ref. section 3.2.3) that

  - part or all of the *defined* object spectrum will become invisible. A re-normalization of the intensity as well as repair of color components is needed to make vision possible.

  - The resulting dynamic range of the spectrum is always wider than the original. This means in the visible spectral range, the energy is less than the original energy. In most cases, the resulting images will be too dim to view. Intensity compensation of a different type than the one above is necessary to restore the visibility of the images.

[9] In either S or the S'.

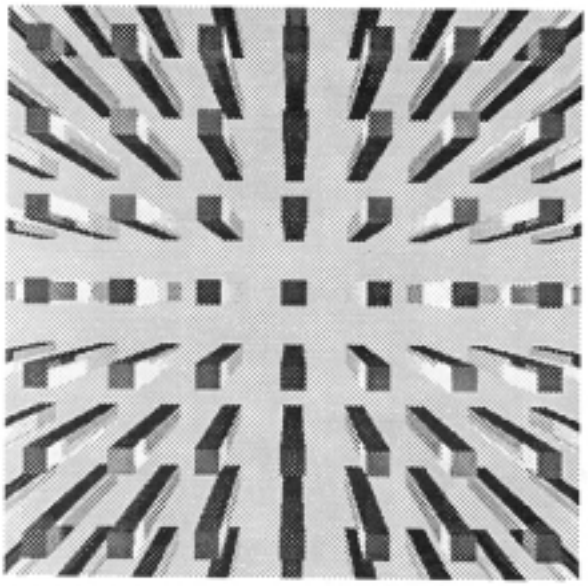

Figure 9: Array of bars viewed at $\beta = 0.0$ (©1989 Hsiung, Dunn & Loofbourrow)

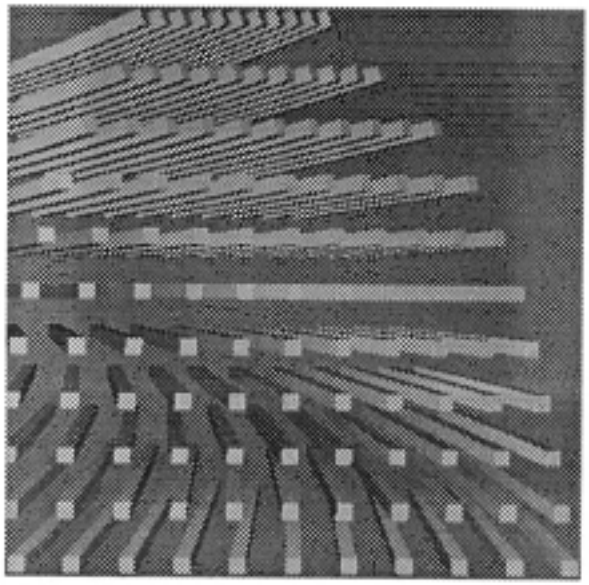

Figure 10: Bar rows with incremental sideways speeds from bottom to top (©1989 Hsiung & Loofbourrow)

We have completed our initial investigation and software implementation to simulate (power spectral based) relativistic Doppler shift. Our work in this area will be reported in a future paper.

5 Conclusion and future work

The *REST-frame* algorithm is a construct used for the study of nature. It is a new analytical tool which moves beyond the root mathematical language of modern physics by means of an interactive exploratory visualization methodology. The *REST-frame* algorithm allows us to create an environment for empirical simulation. This methodology is a preliminary step towards expanding the conceptual building-blocks with which we perceive the world as well as towards increasing the visionary capacity of the mind.

We submit that this visualization tool and the associated techniques could have far-reaching impact on future research in such diverse fields as the following: cosmology, nuclear science, space science and exploration, cognitive science and perceptual studies, computer micro-architecture and networks. Further work may involve the simulation of visual effects in accelerated frames of reference and in animation studies of macroscopic and microscopic domains.

Acknowledgments

We would like to thank Nathan Loofbourrow and Michael Wu for their assistance. Thanks are also due to Robert H. P. Dunn for his profound ideas about this research. We are grateful to Kathryn Porsche for her insightful suggestions that contributed to this presentation.

References

[1] R. Cook and K. Torrance. A reflectance model for computer graphics. *ACM Trans. Graphics*, 1(1):7–24, Jan 1982.

[2] Andrew Glassner. *An Introduction to Ray-Tracing*. Academic Press Limited, 1989.

[3] R. Goldstein and R. Nagel. 3-D visual simulation. *Simulation*, 25, 1971.

[4] Ping-Kang Hsiung. Data structures for ray-tracing. *Thesis Proposal, Carnegie Mellon University*, Feb. 1989.

[5] Ping-Kang Hsiung and Robert H. P. Dunn. Visualizing relativistic effects in spacetime. In *Proceedings of the Supercomputing '89 Conference*, Nov. 13-17, 1989.

[6] Ping-Kang Hsiung and Robert H. Thibadeau. Spacetime visualization of 3D relativistic motion. *Unpublished document*, Oct., 1989.

[7] Ping-Kang Hsiung, Robert H. Thibadeau, and Michael Wu. T-buffer: fast visualization of relativistic effects in spacetime. In *1990 Symposium on Interactive 3D Graphics (to appear)*, March 18-21, 1990.

[8] T.L. Kay and J.T. Kajiya. Ray tracing complex scenes. *Computer Graphics (SIGGRAPH)*, 269–278, Aug. 1986.

[9] C. Møller. *The Theory of Relativity*. Oxford University Press, 1960.

[10] R. Penrose. The apparent shape of a relativistically moving sphere. *Proceedings of the Cambridge Philosophical Society*, 55:137–9, July 29 1958.

[11] Bui Phong. Illumination for computer generated pictures. *CACM*, 18(6):311, June 1975.

[12] Robert Resnick. *Introduction to Special Relativity*. Rensselaer Polytechnic Institute, 1968.

[13] E. Taylor and J. Wheeler. *Spacetime Physics*. M.I.T. / Princeton, 1966.

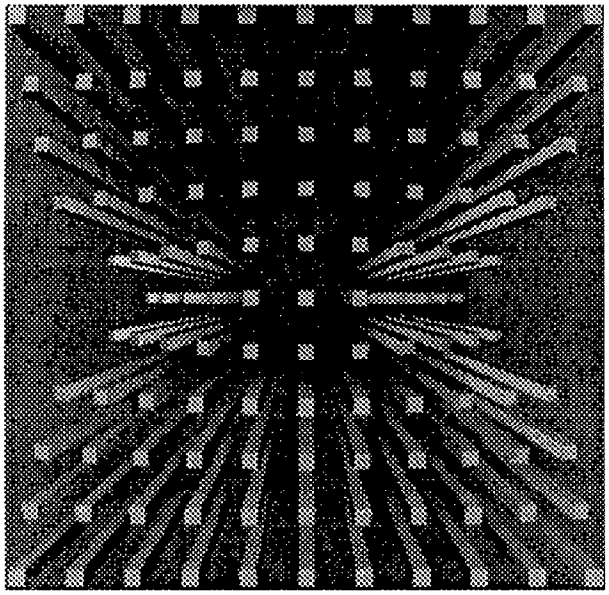

Figure 11: Bar rows with varying speeds towards observer; see text (©1989 Hsiung & Loofbourrow)

[14] J. Terrell. Invisibility of the Lorentz contraction. *Physical Review*, 116(4):1041, 1959.

[15] K. E. Torrance and E. M. Sparrow. Theory for off-specular reflection from rougheded surfaces. *Journal of the Optical Society of America*, 1105, 1967.

[16] V.F. Weisskopf. The visual appearance of rapidly moving bodies (section). *Physics Today*, 13(9):24, 1960.

[17] T. Whitted. An improved illumination model for shaded display. *CACM*, 343–349, June 1980.

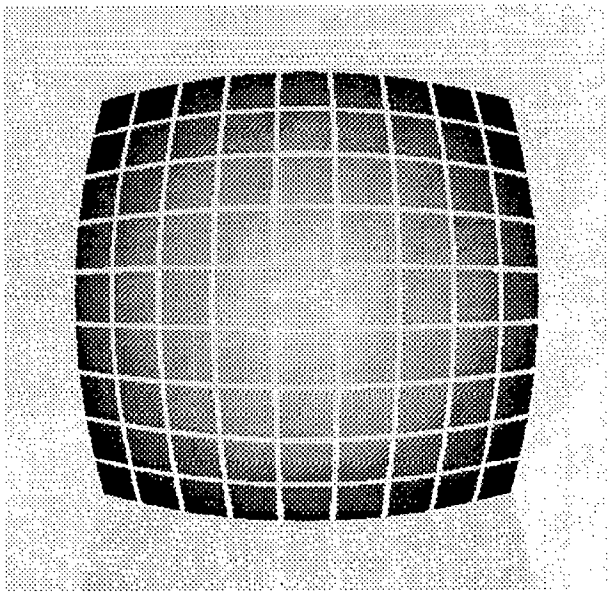

Figure 12: Doppler shift: objects traveling towards observer at 0.9c (©1989 Hsiung)

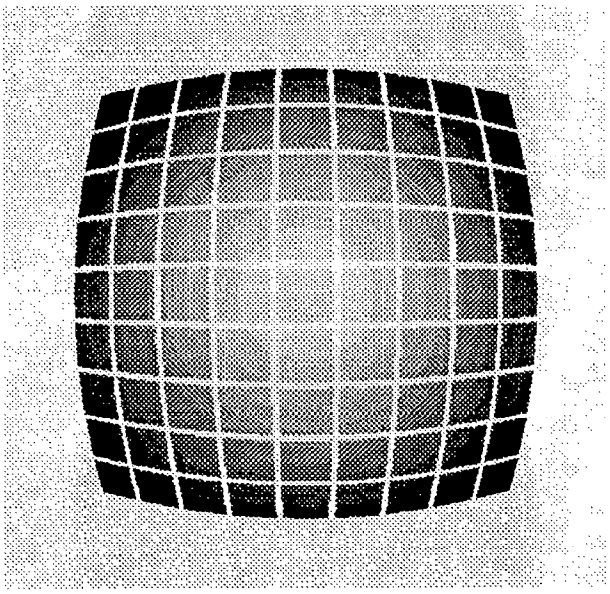

Figure 13: Doppler shift (quantized): objects traveling towards observer at 0.9c (©1989 Hsiung)

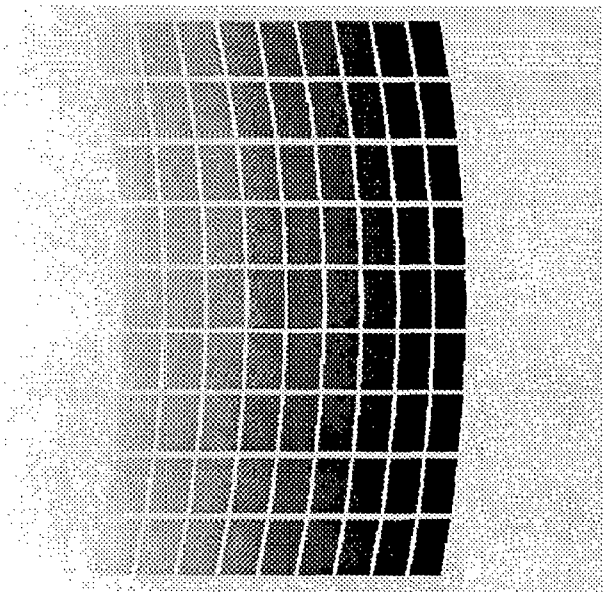

Figure 14: Doppler shift: transverse objects traveling at 0.8c (©1989 Hsiung)

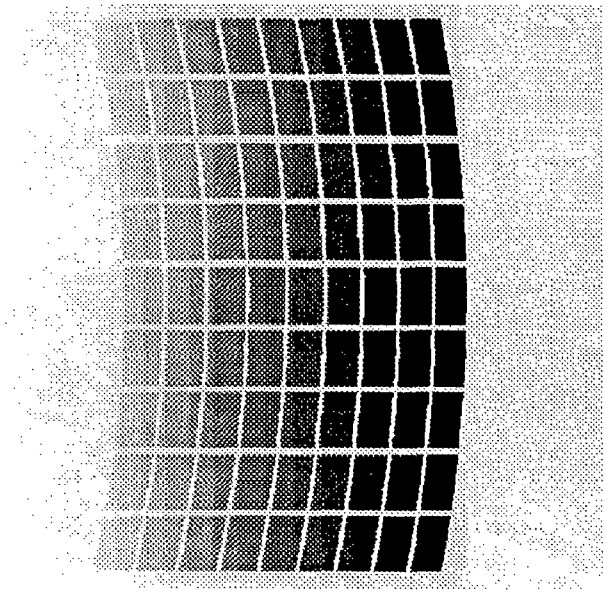

Figure 15: Doppler shift (quantized): transverse objects traveling at 0.8c (©1989 Hsiung)